# Lecture 7: The El Niño Phenomenon

Henk A. Dijkstra; notes by Tom Eaves & Anna FitzMaurice

June 23, 2015

## 1  Phenomenology of El Niño Southern Oscillation

In its mean state, there is strong zonal asymmetry in the equatorial Pacific. The climatological mean easterly trade winds pile up warm water in the western Pacific, whilst cool water is upwelled in the east due to Ekman divergence there, as depicted in Figure 1. Corresponding to this zonal temperature gradient is a sea surface height (SSH) gradient, with high SSH in the west and low SSH in the east. The SSH gradient is compensated at depth by a depressed thermocline in the west, and a shallower thermocline in the east. We have good measurements of the equatorial Pacific from the TAO/TRITON array of approximately 70 moored ocean buoys, which have been monitoring surface and subsurface temperatures, wind speed and direction, and precipitation since 1994.

Every four to seven years, the western Pacific warm pool spreads eastward in a phenomenon known as *El Niño*. This sea surface temperature (SST) anomaly is associated with the eastward propagation of a subsurface temperature anomaly, which in turn is related to a shoaling of the western Pacific thermocline and a depression of eastern Pacific thermocline. These temperature anomalies are coincident with a weakening of the Walker circulation (the zonal circulation cell over the equatorial Pacific), and a shift of the region of highest precipitation to follow the maximum SSTs. The opposite of the El Niño state (i.e. a heightened "normal" state) is referred to as La Niña conditions, and the largescale temperature, pressure, and precipitation, anomalies associated with transitions between El Niño and La Niña states are together known as El Niño Southern Oscillation (ENSO). The El Niño and La Niña phases are shown schematically in Figure 2.

The index used to describe ENSO is an average of the SST anomaly over a region of the equatorial Pacific. Figure 3 shows a timeseries of the ENSO index for the NINO3 region of the eastern Pacific, which spans the region 150W to 90W, between 5S and 5N. A power series decomposition of this timeseries reveals a spectral peak centered about a period of 3 years.

## 2  The Zebiak & Cane model

To capture the oscillatory behavior of ENSO dynamically, a coupled atmosphere-ocean model is required, which admits feedbacks between perturbations to the equatorial easterlies, the thermocline depth, and equatorial SSTs, and as such allows the spontaneous growth of anomalies. We shall also see that oceanic wave dynamics are important to the development and decay of El Niños, and so necessary in a minimal model of ENSO.
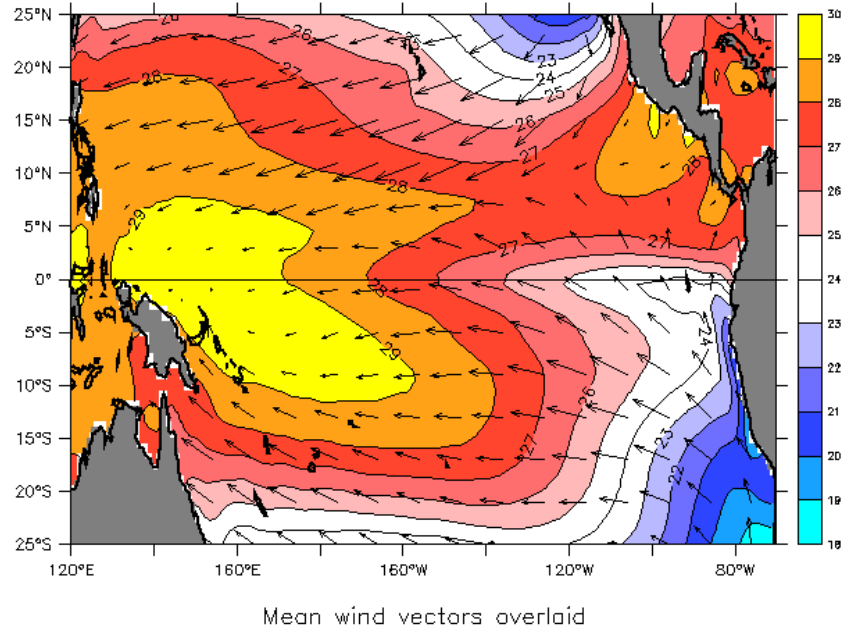
Sea surface temperature in the tropical Pacific

Mean wind vectors overlaid

Figure 1: The climatological mean SST and wind stress in the tropical Pacific. [Reproduced from faculty.washington.edu/kessler.]
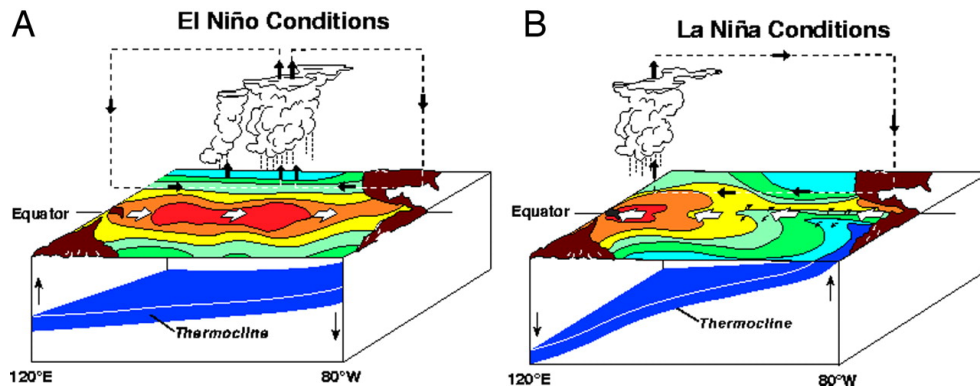


Figure 2: A schematic of (A) El Niño and (B) La Niña states of the tropical Pacfic. [Reproduced from www.noaa.gov.]

## 2.1 Model formulation

Zebiak & Cane (1987), hereon ZC, consider a $1\frac{1}{2}$-layer reduced gravity ocean (depicted in Figure 4) below a constant-depth mixed layer of temperature $T$, which feels a temperature-
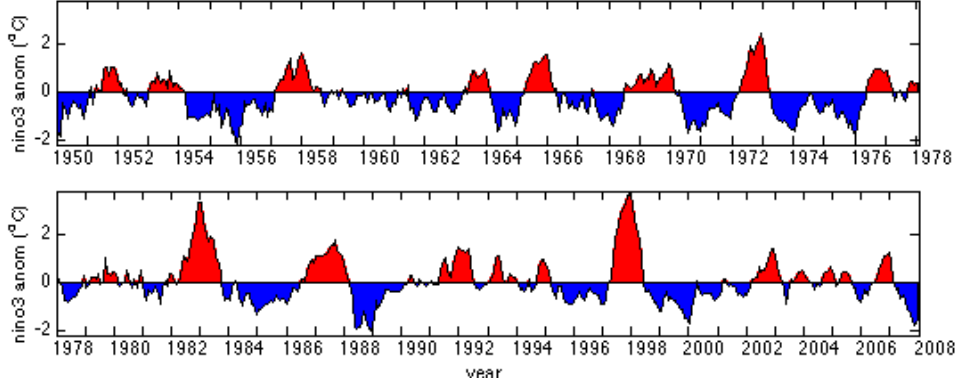
Figure 3: A timeseries of the NINO3 SST anomaly, with El Niño events colored in red and La Niña events colored in blue. [Reproduced from http://www.seas.harvard.edu/climate.]

dependent wind stress

$$\tau^x = \tau^x_{\text{ext}} + \mu \mathcal{A}(T - T_0), \tag{1}$$

for some atmospheric operator $\mathcal{A}$, and coupling parameter $\mu$ (with $\mu = 0$ corresponding to the entirely uncoupled case, and $\mu = 1$ describing "normal" coupling).

The reduced gravity ocean model equations for the horizontal velocities $(u, v)$ and depth $h$ are

$$\frac{\partial u_1}{\partial t} - \beta_0 y v_1 = -g' \frac{\partial h}{\partial x} + \frac{\tau^x}{\rho h}, \tag{2}$$

$$\beta_0 y u_1 = -g' \frac{\partial h}{\partial y}, \tag{3}$$

$$\frac{\partial h}{\partial t} = -H \left( \frac{\partial u_1}{\partial x} + \frac{\partial v_1}{\partial y} \right), \tag{4}$$

$$x = 0 : \int_{-\infty}^{\infty} u_1(y) dy = 0, \tag{5}$$

$$x = L : u_1 = 0, \tag{6}$$

$$y \to \pm\infty : u_1, v_1, h, \text{ bounded}, \tag{7}$$

in the upper layer, and zero velocities in the lower layer.

The evolution of the mixed layer temperature $T$ is governed by an advection-diffusion equation with relaxation back to some atmospheric temperature $T_0$, and relaxation to a specified subsurface temperature profile $T_s(h)$ in the presence of upwelling $w > 0$, as follows

$$\frac{\partial T}{\partial t} + u_1 \frac{\partial T}{\partial x} + v_1 \frac{\partial T}{\partial y} + w_1 \mathcal{H}(w_1) \frac{T - T_s(h)}{H} + \alpha_T (T - T_0) - \kappa_H \nabla^2 T = 0, \tag{8}$$

where $\mathcal{H}$ is the Heaviside function, along with boundary conditions

$$x = 0, L : \frac{\partial T}{\partial x} = 0, \tag{9}$$
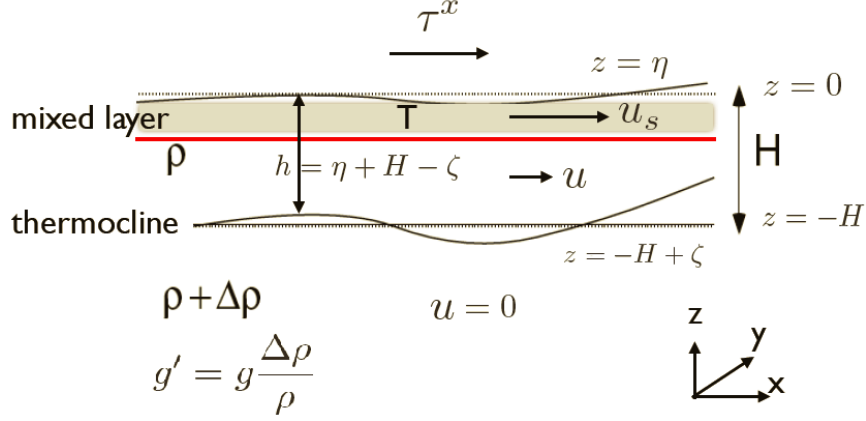
$$y \to \pm\infty : T \text{ bounded}. \tag{10}$$

Figure 4: The ocean component of the ZC model. A thermocline of density $\rho$ overlies a denser stationary layer of density $\rho + \Delta\rho$. The ocean feels atmospheric wind stress and temperature through constant depth mixed layer of temperature $T$.

## 2.2 Wave dynamics in the ZC ocean model

Consider free waves with $\tau_x = 0$, corresponding to no wind stress input, and no coupling with the mixed layer temperature field $T$. Let $u = \hat{u}(y)e^{i(kx-\sigma t)}$ and define $v$ and $h$ similarly. Then,

$$-i\sigma\hat{u} - \beta_0 y\hat{v} = -ikg'\hat{h}, \tag{11}$$

$$\beta_0 y\hat{u} = -g'\hat{h}', \tag{12}$$

$$-i\sigma\hat{h} + H(ik\hat{u} + \hat{v}') = 0. \tag{13}$$

Look first for solutions with $\hat{v} = 0$. Then,

$$-\sigma\hat{u} = -g'k\hat{h}, \tag{14}$$

$$-\sigma\hat{h} + Hk\hat{u} = 0, \tag{15}$$

$$\tag{16}$$

which has a non-zero solution only if

$$\sigma^2 = k^2 g'H, \tag{17}$$

and so

$$\frac{\sigma}{k} = \pm\sqrt{g'H} \equiv \pm c_0. \tag{18}$$

We can also solve for $\hat{h}$ and $\hat{u}$, since

$$\beta_0 y\hat{u} = \frac{\beta_0 y g'k\hat{h}}{\sigma} = -g'\hat{h}', \tag{19}$$

and so

$$\hat{h}(y) = \hat{h}(0)\exp\left[-\frac{\beta_0 k}{2\sigma}y^2\right] \equiv \hat{h}(0)\exp\left[-\frac{1}{2}\left(\frac{y}{\lambda_0}\right)^2\right], \tag{20}$$

where $\lambda_0 = \sqrt{c_0/\beta_0}$ is the Rossby deformation radius. Note that for $\hat{h}(y)$ to be bounded as $y \to \pm\infty$ we have set $\sigma/k = +c_0$.

We can solve for the general case $\hat{v} \neq 0$ by using the Hermite polynomials $H_n$, in which case

$$\hat{u}_j(y) = \frac{1}{2\sqrt{2}} \left( \frac{\psi_{j+1}(y)}{\sqrt{j+1}} - \frac{\psi_{j-1}(y)}{\sqrt{j}} \right), \tag{21}$$

$$\hat{h}_j(y) = \frac{1}{2\sqrt{2}} \left( \frac{\psi_{j+1}(y)}{\sqrt{j+1}} + \frac{\psi_{j-1}(y)}{\sqrt{j}} \right), \tag{22}$$

$$\hat{v}_j(y) = \psi_j(y), \tag{23}$$

where

$$\psi_j(y) = \frac{H_j(y/\lambda_0) \exp[-(y/\lambda_0)^2/2]}{(2^j j! \pi^{1/2})^{1/2}}, \tag{24}$$

and the corresponding phase speeds are

$$c_j = -\frac{c_0}{2j+1}. \tag{25}$$

## 2.3   Possible feedbacks in the ZC model

To explore the feedbacks possible in the full model, consider a perturbation (denoted by hats) to some steady state (denoted by overbars) of the simplified temperature equation

$$\frac{\partial T}{\partial t} = -w \frac{T - T_s(h)}{H}. \tag{26}$$

Linearizing about the steady state, this becomes

$$\frac{\partial \hat{T}}{\partial t} = -\hat{w} \frac{\bar{T} - T_s(\bar{h})}{H} - \bar{w} \frac{\hat{T} - T_s'(\bar{h})\hat{h}}{H}. \tag{27}$$

Now it can be seen that if there is a warm anomaly in the mixed layer (i.e. $\hat{T} > 0$) giving rise to a deepening of the thermocline (i.e. $\hat{h} > 0$), the second term on the right of equation 27 will be positive, leading to more warming. This positive feedback is known as the *thermocline feedback*. Similarly, from the first term on the right of equation 27, it can be deduced that a positive temperature anomaly, associated with a reduction in upwelling ($\hat{w} < 0$), will likewise enhance the positive temperature anomaly, acting as a positive feedback. This is called the *upwelling feedback*.

An analogous treatment of the zonal advection terms of the temperature equation

$$\frac{\partial T}{\partial t} = -u \frac{\partial T}{\partial x} \tag{28}$$

yields linearized equation

$$\frac{\partial \hat{T}}{\partial t} = -\bar{u} \frac{\partial \hat{T}}{\partial x} - \hat{u} \frac{\partial \bar{T}}{\partial x}. \tag{29}$$

Now a positive temperature anomaly will produce a zonal velocity anomaly $\hat{u}$ that acts to enhance this anomaly by the advection of the mean temperature field $\bar{T}$. This is the *zonal advection feedback*.

## 2.4 ZC model equilibria, stability, and bifurcations

After discretisation, we can reduce the ZC model to the general form

$$\frac{\mathbf{x}}{dt} = \mathbf{f}(\mathbf{x}, \mu). \tag{30}$$

Then, equilibria $\mathbf{x} = \mathbf{x}^*$ are found by solving

$$\mathbf{f}(\mathbf{x}^*, \mu) = 0. \tag{31}$$

Suppose that we know one solution $\mathbf{x}^*(\mu = 0)$. As $\mu$ is varied, we expect $\mathbf{x}^*(\mu)$ to vary continuously (at least for a while, generically). Such a branch of solutions traces out a curve in the $\mathbf{x}$-$\mu$ plane. A convenient way to solve such a system is to utilise this continuous changing of the solutions by viewing the arclength $s$ along this curve as a parameter and solve instead

$$\mathbf{f}(\mathbf{x}^*(s), \mu(s)) = 0, \tag{32}$$

$$\mathcal{N}\left(\frac{\mathbf{x}^*}{ds}, \frac{\mu}{ds}\right) = 0, \tag{33}$$

where $\mathcal{N}$ is a normalisation constraint on the arclength.

Given an equilibria $\mathbf{x}^*$, we are interested in its stability. For this purpose, write $\mathbf{x} = \mathbf{x}^* + \mathbf{x}'$. Then, linearising in $\mathbf{x}'$, the equation becomes

$$\frac{\mathbf{x}'}{dt} = J\mathbf{x}', \tag{34}$$

where $J_{ij} = \partial f_j / \partial x_j(\mathbf{x}^*(\mu))$ is the Jacobian of the dynamical system evaluated at $\mathbf{x} = \mathbf{x}^*(\mu)$.

We can determine the stability of a given solution $\mathbf{x}^*$ by writing $\mathbf{x}' = \hat{\mathbf{x}}e^{\sigma t}$, and then $\sigma$ satisfies the eigenvalue problem

$$J\hat{\mathbf{x}} = \sigma\hat{\mathbf{x}}. \tag{35}$$

We say that $\mathbf{x}^*$ is a stable equilibria if $\mathbb{R}(\sigma) < 0$ and an unstable equilibria if $\mathbb{R}(\sigma) > 0$.

As $\mu$ is varied, there are a number of possibilities for the behaviour of such equilibria. In general there will be particular values of $\mu = \mu^*$, called *bifurcation* points, at which a given solution changes its stability properties, or ceases to exist altogether, as $\mu$ is varied through its bifurcation value $\mu^*$. There a four canonical types of bifurcations found in dynamical systems, namely

- **Saddle–node bifurcation:** A saddle–node bifurcation is the bifurcation in which there are no equilibria for $\mu < \mu^*$ and a pair of equilibria with opposite stability properties for $\mu > \mu^*$. Through a change of variables, any one-dimensional system with a saddle–node bifurcation can be mapped, sufficiently close to its bifurcation point, onto the form

$$\dot{x} = \mu - x^2. \tag{36}$$

  We see that for $\mu < 0$ there are no equilibria, whilst for $\mu > 0$ there are two equilibria $x^* = \pm\sqrt{\mu}$. The Jacobian is just $-2x$, and so the solution $x^* = \sqrt{\mu}$ is stable, whilst the solution $x^* = -\sqrt{\mu}$ is unstable.

- **Pitchfork bifurcation:** A pitchfork bifurcation is the bifurcation in which there is a single equilibria (which may or may not be stable) for $\mu \lessgtr \mu^*$ (the case $<$ is called supercritical, and the case $>$ is called subcritical), and three equilibria for $\mu \gtrless \mu^*$ in which the original equilibria point swaps its stability, and the two new equilibria have the stability of the original solution. The normal form for a pitchfork bifurcation is

$$\dot{x} = \mu x - x^3 \quad \text{(supercritical)}, \tag{37}$$

$$\dot{x} = \mu x + x^3 \quad \text{(subcritical)}. \tag{38}$$

In the first case, the solution $x = 0$ is stable for $\mu < 0$ and unstable for $\mu > 0$, and the solutions $x = \pm\sqrt{\mu}$ only exist for $\mu > 0$, and are stable there. In the second case, the solution $x = 0$ is stable for $\mu < 0$ and unstable for $\mu > 0$, and the solutions $x = \pm\sqrt{-\mu}$ only exist for $\mu < 0$ and are unstable there. The transformation $t \mapsto -t$ reverses the stability of all the solutions, but the systems still retain their original labels 'supercritical' and 'subcritical'.

- **Transcritical bifurcation:** A transcritical bifurcation is the bifurcation in which there are two solutions for each of $\mu \lessgtr \mu^*$, but at $\mu = \mu^*$ they coincide, and swap their stability. The normal form for a transcritical bifurcation is

$$\dot{x} = \mu x - x^2. \tag{39}$$

We see that the equilibria are always $x = 0$ or $\mu$. However, the Jacobian is $\mu - 2x$, and so the solution $x = 0$ is stable for $\mu < 0$ and unstable for $\mu > 0$ whereas the solution $x = \mu$ is unstable for $\mu < 0$ and stable for $\mu > 0$.

- **Hopf bifurcation:** A Hopf bifurcation is the bifurcation in which there is one equilibria for $\mu \lessgtr \mu^*$ (which we again call super/subcritical), and a single equilibria for $\mu \gtrless \mu^*$ with the opposite stability, and a periodic orbit that coincides with the equilibria when $\mu = \mu^*$. The normal form for a Hopf bifurcation is

$$\dot{x} = \mu x - \omega y - x(x^2 + y^2), \tag{40}$$

$$\dot{y} = \mu y + \omega x - y(x^2 + y^2). \tag{41}$$

It is clear that $(x, y) = (0, 0)$ is an equilibria for this system. The Jacobian at $(0, 0)$ is

$$J(0,0) = \begin{pmatrix} \mu & -\omega \\ \omega & \mu \end{pmatrix}, \tag{42}$$

which has eigenvalues $\sigma = \mu \pm i\omega$, and so the equilibria $(x, y) = (0, 0)$ is stable for $\mu < 0$ and unstable for $\mu > 0$.

To demonstrate that this system has a periodic orbit for $\mu > 0$ it is convenient to use polar co-ordinates $(x, y) = r(\cos\theta, \sin\theta)$, in which case

$$\dot{r} = \mu r - r^3, \tag{43}$$

$$\dot{\theta} = \omega, \tag{44}$$

and so provided $\omega \neq 0$, there is a stable periodic orbit solution $r = \sqrt{\mu}$ and $\theta = \omega t + \theta_0$ when $\mu > 0$. Note that in the degenerate case $\omega = 0$, we obtain a circle of fixed points that are marginally stable in the angular direction, and stable in the radial direction. Since the equation for $r$ is nearly pitchfork-like (we don't allow $r < 0$), changing the signs of terms in the above equations yields super/subcritical Hopf bifurcations with the same convention as for the pitchfork case.

A Hopf bifurcation can be viewed physically as feedbacks amplifying to give an oscillatory signal.

There are a whole range of other bifurcations which are typically degenerate cases in which the first order nonlinearity occurs at even higher orders in $x$. We typically don't see these, and indeed typically don't see pitchfork or transcritical bifurcations. The reason for this is that, for example, if we have made some error in modeling whatever physical system we are interested in, then perhaps each of the equations for these bifurcations should have an extra constant $\epsilon$ added to the right hand side. Then we see that the saddle–node bifurcation remains a saddle–node bifurcation, the Hopf bifurcation remains a Hopf bifurcation, but the pitchfork bifurcation separates into an isolated non-bifurcating solution and a saddle–node bifurcation, and the transcritical bifurcation separates into a pair of saddle–node bifurcations.

For higher dimensional dynamical systems, we may invoke the centre manifold theorem (which is quite technical) to see that near a bifurcation point, the dynamics of the dynamical system collapses onto a low dimensional (often one or two) manifold on which the reduced dynamics generically take the form of one of the bifurcations discussed above.

## 2.5 Hopf bifurcation in the ZC model

As the ocean–atmosphere coupling parameter $\mu$ in the ZC model is increased from zero, there has been shown to be a Hopf bifurcation when $\mu \approx 0.525$, and the period of the resulting periodic orbit is approximately 4 years. This observation has been used as a first order explanation of El Niño. Additionally, it is known that $\mu$ scales with the square of ocean basin size, and so, for example, given that the size of the Atlantic ocean basin is approximately one third of the size of the Pacific ocean basin, we have $\mu_{\text{Atlantic}} \approx \mu_{\text{Pacific}}/9$, and so the lack of an El Niño event in the Atlantic could be explained by the fact that $\mu_{\text{Atlantic}} \lesssim 0.525 \lesssim \mu_{\text{Pacific}}$, and so there does not exist a periodic orbit solution of the ZC model.

For the ZC model, the Hopf bifurcation corresponds to an amplifying feedback of geometrically confined Rossby and Kelvin basin modes with SST modes.

# 3 Physical Mechanisms for ENSO

We have seen from the ZC model that with idealized ocean-atmosphere coupling and oceanic wave dynamics it is possible to find oscillatory solutions in certain parts of parameter space that resemble ENSO in amplitude and period. Below we heuristically describe two mechanisms that might give rise to such oscillatory behavior.

## 3.1 Wave oscillator

Consider a positive temperature anomaly at the equator in the Pacific ocean, which corresponds to a positive SSH anomaly on-equator, with compensatory negative SSH anomalies off-equator to the north and south. We have seen that such a signal may propagate eastwards as an equatorial Kelvin wave on the equator, which may be interpreted as the eastward propagating and growth of an El Niño. Meanwhile, the off-equator signal will propagate westward as a Rossby wave and, on reaching the westerward basin boundary, may be reflected as an equatorial Kelvin wave. This reflected wave signal has the possibility of interfering with and killing the original positive temperature anomaly, ending the El Niño. Whilst this delayed oscillator mechanism of El Niño undoubtedly influences ENSO dynamics, a consideration of the timescales involved (from the Kelvin and Rossby wave speeds) does not explain the observed ENSO period of four to seven years.
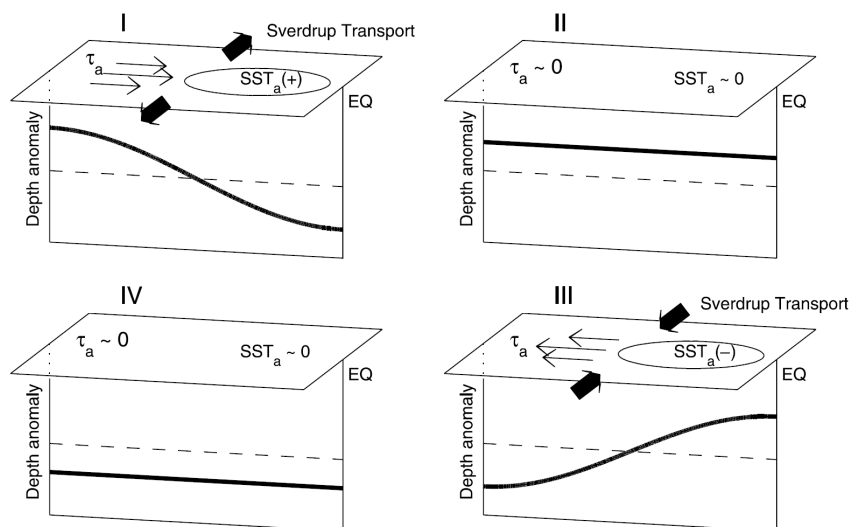
## 3.2 Recharge oscillator



Figure 5: A schematic of the stages of the recharge oscillator mechanism for ENSO.

An alternative mechanism that produces longer timescale variability comes from considering the overall basin adjustment. A positive SST anomaly in the eastern Pacific will produce a westerly wind stress anomaly. The wind stress acts to change the thermocline slope, piling up water and so depressing the thermocline in the east, whilst shoaling the thermocline in the west. Such a perturbation to the thermocline slope will enhance the SST perturbation, acting as a positive feedback. As the positive temperature anomaly strengthens, there is a divergent transport of heat off-equator by the ocean, which shoals the thermocline, suppressing the SST anomaly and so reducing the westerly wind anomaly. The shoaling of the thermocline eventually carries the system into the opposite phase, with a negative SST anomaly in the east, and so an easterly wind stress anomaly. This causes the convergent transport of heat to the equator, resulting in the "recharge" of the ocean

heat content there. As such, this mechanism is known as the *recharge oscillator* view of ENSO. This process is shown schematically in Figure 5.